

## Anomalous Variation of the Ocean's Inertial Oscillations at the Hawaii Shelf

Academician V. G. Bondur, K. D. Sabinin, and Yu. V. Grebenyuk

Received December 12, 2012

**Abstract**—The data of acoustic Doppler profilometers placed at the edge of the steep shelf of Oahu Island, Hawaii, are analyzed for the currents. The specific character of inertial oscillations is revealed in the region: strong elongation of inertial orbits, a large amount of anomalous (cyclonic) current rotation, and sharp weakening in the divergence layer of the background (low-frequency) oscillations, the strong variation of which results in significant deviations of the effective inertial frequency from its local geographical value. It is suggested that cyclonic rotation of the inertial currents is related to a strong decrease in the effective oscillation frequency of the oceanic waves on the shelf.

DOI: 10.1134/S1028334X13050012

The inertial oscillations playing a key role in energy transfer and mixing of the oceanic waters represent circular water rotation with the sun with a period, which changes with latitude  $\varphi$  as  $12/\sin\varphi$ , of an hour. Near the steep slopes and under the effect of strong and heterogeneous currents, both the shape and the period of these oscillations may vary significantly. All of this is strikingly manifested in Mamala Bay (Oahu Island, Hawaii), where the steep shelf transits into an almost vertical island slope and strong variable currents are observed. The anthropogenic impacts on the ecosystems of the coastal water areas have been studied in this area for several years [1–6]. The data of different years from the bottom acoustic Doppler profilometers of the currents (ADP) [7], strongly different in wind conditions and density water stratification, were used for analysis of the peculiarities and variability of the inertial oscillations in this region. The ADP were placed along the shelf edge at a depth of about 80 m at three points at a distance of approximately 3 km from each other [1–7]. The zonal (U), longitudinal (V), and vertical (W) components of the current velocities were measured in August–September every minute for 512 h in 2003 and 385 h in 2004 and every 2 m from 4 to 76 m. The strong (up to 1 m/s) westward transfer caused by a typhoon that passed close by was observed in the upper 12-m layer in 2003, whereas an obvious but much weaker southwestern flow did not penetrate deeper than 4 m in 2004 [1, 2]. The location and the form of the pycnocline varied strongly due to internal tides. During the measurements in 2003, the pycnocline began at the bottom, on average, while in 2004 its

core with maximum buoyancy frequency of  $\sim 15$  cycles/hour was notably higher at 50 m [2, 4, 6].

The application of the averaging of periodograms by frequencies commonly used had no sense during the spectral analysis of experimental data, because the planetary inertial frequency of 0.03 cycles/hour in the studied region is lower only for 0.01 cycles/hour than the well-expressed day internal tides. Thus, to increase the reliability of spectral estimations, we averaged the periodograms by the velocity components at two measurement points at a distance of approximately 3 km from each other [1–7]. We analyzed the variations of spectra of the mean-square current amplitudes calculated by these estimations with the depth (Fig. 1) and also the average values and spectra ratios of the right and left rotations of the current vector in the upper 10-m layer, where the most intensive oscillations were observed, as tends to occur with wind generation of inertial waves [8].

Even in spectra with temporal ranges of 512 hours, which distinguish the inertial and daily oscillations, the latter are manifested much more strongly than the inertial ones (Fig. 1). Only the dominant right current rotation near the inertial frequency allows consideration of the inertial and daily oscillations separately. With respect to this, for further analysis, the experimental data were processed with a band pass Butterworth filter of the third order, which suppresses by more than two times the oscillations at frequencies lower than 0.025 and higher than 0.035 cycles/hour and transmits in its true value the oscillations with frequency close to the local inertial period of 0.03 cycles/hour [1, 2].

The intensity variability of inertial oscillations may be inferred from the variations in the mean-square amplitude of the rotation constituent of the current field in the inertial frequency range, because precisely

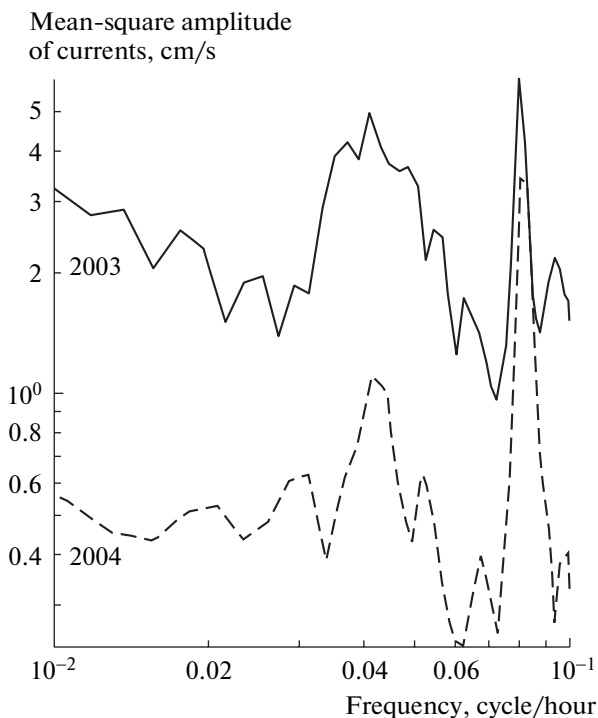


Fig. 1. Average spectra of the mean-square amplitudes in the upper layer of the ocean in 2003 and 2004.

this rotation is typical for inertial waves [9]. The mean-square amplitude was calculated using the dispersion of the rotation constituent in the band of the spectral analysis  $\frac{1}{2n}$  wide, which is  $Drot = \frac{|D|}{2n}$ , where  $D$  is the

spectral rotation invariant [10] and  $n$  is the length of the analyzed row.

Thus, the amplitude, taking into account the rotation sign ( $sgn D$ ), is  $Arot = \sqrt{Drot} \cdot sgn D$ . Having calculated the current spectra of the amplitude and ratios of the ellipsis axes of the inertial waves for all measurement horizons by 64-hour segments with a shift in 1 hour, we obtained 34 000 and 26 418 estimations of the ellipsis parameters in 2003 and 2004, respectively. The revealed strong weakening of inertial currents in 2004 and unexpectedly large abundance of the left-side (cyclonic) rotation are uncommon for inertial oscillations. The most intensive anticyclonic currents were concentrated in the upper layer in 2003 and somewhat deeper in 2004.

The repeatability and intensity of ellipses with variously directed current rotation and strong eccentricity may be deduced well from 2-D histograms, which characterize the amount of cases in the axes ratios/rotation amplitude coordinates. Such histograms were calculated for all data. As an example, Fig. 2 shows 2-D histograms for the data of 2003. It is seen that the ellipses of anticyclonic rotation insignificantly prevail and the stronger they are, the more complete. This tendency increases up to the amplitude of 0.6 m/s, where rather complete ellipses occur (up to half of 128 cases). The oblate ellipses of the weak (0.2–0.3 c/s) rotation amplitude are most widespread. The mean-square amplitude is 0.3 cm/s, and the axes ratio is  $-0.13$  in the repeatability peak (5% of estimations). The mean-square amplitude is 0.16 cm/s, and the axes

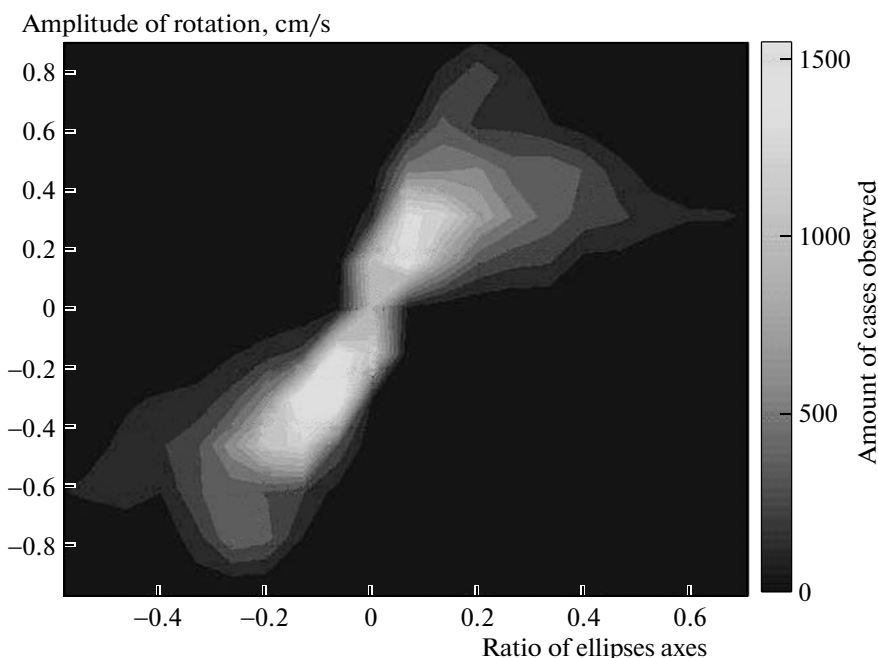
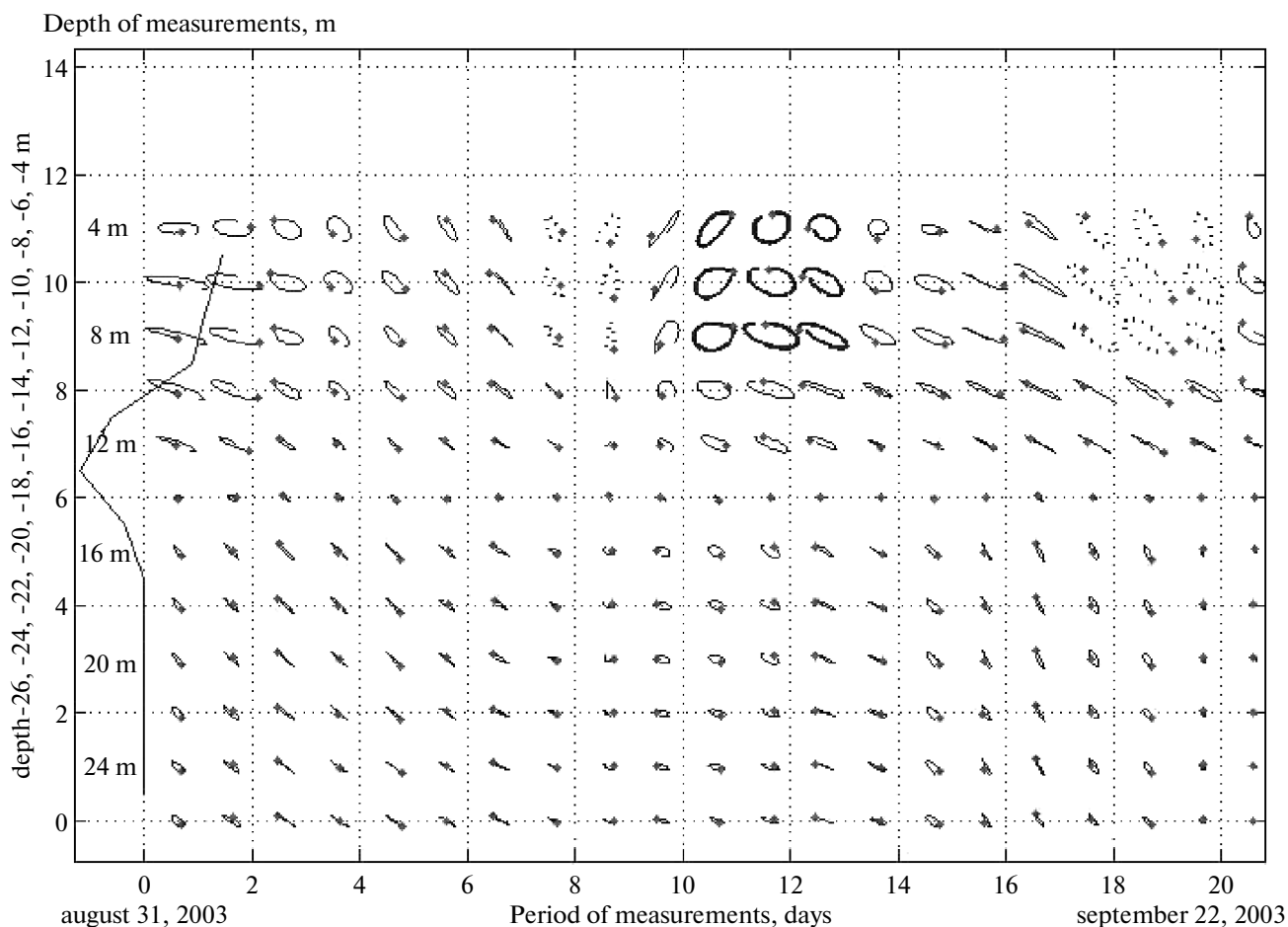


Fig. 2. Two-dimensional histograms of the inertial oscillations (the amount of cases in the axes ratio/rotation amplitude coordinates).



**Fig. 3.** Daily 30-h hodographs of inertial currents (in the conditional scale) in 2003 in time (days)—depth (m) coordinates. The points indicate the initial positions of the velocity vectors. The average convergence profile of horizontal currents (in the units of 50/s) is shown from the left by the thin line on the plot.

ratio is +0.07 in the repeatability peak of cyclonic ellipses (4% of estimations).

The histogram of data of 2004 differs significantly by lesser amplitudes and almost equal repeatability of cyclonic and anticyclonic rotations.

The variation of ellipses in time and along the depth are clearly presented by the hodographs of velocities of inertial currents, the example of which for the data of 2003 is shown in Fig 3. The hodographs (conventionally, orbits) have the shape of ellipses of different amplitudes, characterized by the rotation sign, eccentricity, and orientation. It is obvious from Fig. 3 that the currents in the reviewed frequency range are weak in the beginning of the measurement period and increase only by the ninth day in the upper layer, forming “plump” and large anticyclonic orbits; the most significant of them are highlighted in bold in the figure.

At the end of the measurement period, the rotation becomes cyclonic (the greatest orbits are marked by a dash) and the current orbits are open, which indicates the more than 30-hour period of corresponding oscil-

lations. At the same station, the orbits of inertial currents in 2004 were considerably weaker (by 4–5 times) and less stable, often becoming very narrow. The general picture of the orbit variability in 2003 is similar at two stations at a distance of approximately 3 km, excluding the absence of visible inertial currents at the beginning of the measurements. The strong oscillation weakening in the layer around the 14-m horizon is worth noting, where we observe the discrepancy in the background horizontal currents. Taking into account that convergence of the horizontal currents (Conv) may be estimated from the vertical gradient of the vertical velocity ( $\text{Conv} = -U_x - V_y = W_z$ , where  $U_x$ ,  $V_y$ , and  $W_z$  are the particular derivatives of the velocity components by the  $x$ ,  $y$ , and  $z$  axes), the profile of the average convergence shown in Fig. 3 was calculated in the units of 1/s multiplied at 50 (for agreement with the figure scale). The profile is characterized by large negative values (divergence of the currents) in the layer of 9–15 m, i.e., at those depths in which inertial oscillations are absorbed.

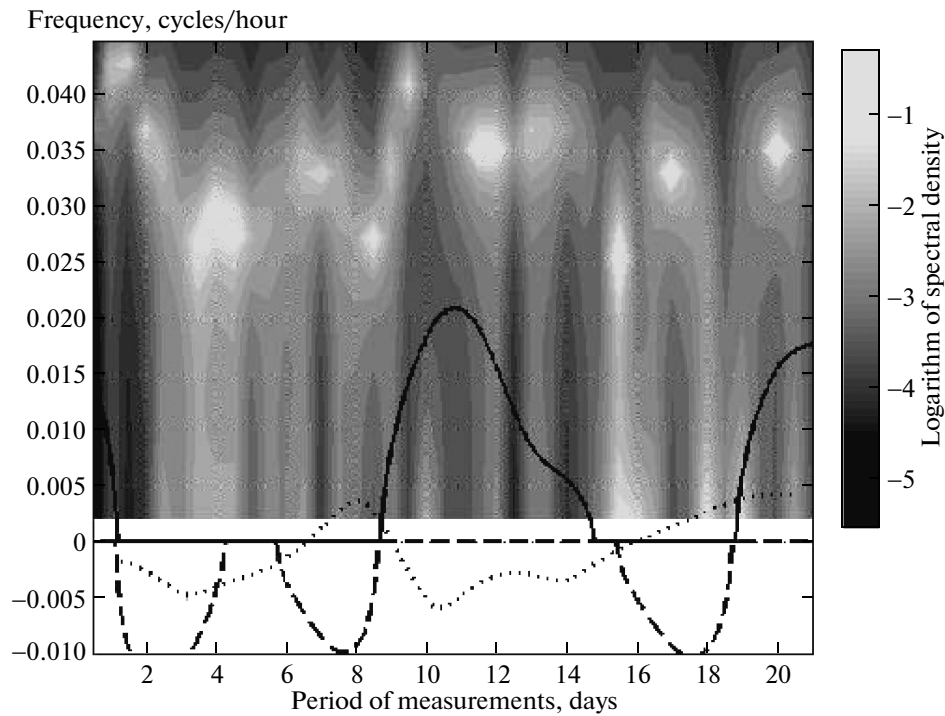


**Fig. 4.** Logarithm of the current spectrum of inertial oscillations of zonal velocity  $U$  at the horizon of 8 m in 2003 (gradations of the gray level). The spectral estimations are calculated by the days with a shift for a half by the high-resolution MUSIC method [12]. The effective frequency  $F_{ef}$  and its supposed values are shown by the bold solid and dashed lines, respectively. The correlation of small and large axes of inertial ellipses, taking into account the rotation sign, is shown by the dotted line (the axes ratio is decreased in 100 times).

In 2004, orbits several times weaker than in 2003 were characterized by stable orientation, elongated along the isobaths. The orbits in the intermediate period of measurements were most stable and covered the entire upper half of the water layer. The currents rotated clockwise almost everywhere, except for the initial measurement period.

Thus far the inertial waves were considered in a narrow frequency range around the planetary inertial frequency at the latitude of the region ( $0.03 \pm 0.005$  cycles/hour). Taking into account the inevitability of the strong effect of the Doppler distortions and the field vorticity of the background currents, it makes sense to somewhat widen the analytical band, applying the Butterworth filter for the frequency band from 0.025 to 0.04 cycles/hour with the estimated dominant right rotation (with the sun) typical of inertial waves. The vorticity effect to the frequency of inertial oscillations may be accounted for by estimation of the effective inertial frequency  $F_{ef}$ , the most complete expression of which is given in [11]:

$$F_{ef} = (f^2 + fV_{ort} - V_xU_y + U_xV_y)^{0.5}, \quad (1)$$

where  $f$  is the circular planetary frequency (in our case,  $f = 6.28 \cdot 0.03$  rad/hour);  $V_{ort} = \frac{\partial V}{\partial x} - \frac{\partial U}{\partial y}$  is the vorticity; and  $\frac{\partial U}{\partial x}$ ,  $\frac{\partial V}{\partial y}$ ,  $\frac{\partial U}{\partial y}$ ,  $\frac{\partial V}{\partial x}$  are the derivatives of compo-

nents of the background currents  $U$  and  $V$  along the  $OX$  and  $OY$  coordinate axes.

The measurements of 2004 at stations located at the same latitude allow calculation of the derivatives  $\frac{\partial U}{\partial x}$  and  $\frac{\partial V}{\partial x}$ . They, however, may be estimated along the longitudinal axis only if the current field variation is suggested in this direction. Assuming a linear reduction of the background components of the velocities  $U$  and  $V$  toward the coast, we found a strong temporal variability of the effective oscillation frequency from 0.021 cycles/hour to the supposed values of 0.013 cycles/hour (Fig. 4).

Such strong variations of the effective frequency of inertial oscillations are caused by the sharp spatial-temporal variability of the background currents, locally leading to the decrease in  $F_{ef}$  down to the supposed values, which may be considered as negative values of the effective frequency with corresponding change in the rotation sign. The sharp decrease in  $F_{ef}$  estimations occurred in the first through fourth, sixth to ninth, and fifteen to nineteenth days of measurements. In the middle of registration, when the inertial orbits were most "correct" (Fig. 3 and the curve of the ellipsis axes ratio in Fig. 4),  $F_{ef}$  reaches maximum values, decreasing to the end of the registration, when the orbits with anomalous rotation appeared.

In spite of certain convention of the estimations of the effective oscillation frequency due to accepted assumptions, they more or less satisfactorily reflect the tendencies of variation in  $F_{ef}$  evident from the obvious (although incomplete) correspondence of variations of estimations of  $F_{ef}F_{ef}$  and the measured frequency of the current spectra peaks (Fig. 4). Fluctuating around the average value of 0.03 cycles/hour, the peak frequency varies significantly, which is in agreement with variations of the effective frequency but considerably exceeds it. When the effective frequency decreases, the spectral density increases at low frequencies, which is natural to interpret as evidence of a corresponding increase in the period of the inertial oscillations. This is clear from the clearly visible open contour of the 30-h orbits near the fourth, eighth, and eighteenth days of measurements.

Based on detailed analysis of the field oscillations of the currents on the Hawaiian shelf, we revealed a significant shape distortion of current velocities, uncommon frequent anomalous rotations related to the strong decrease in the effective inertial oscillation frequency, and sharp weakening of inertial waves in the divergence layer of the background horizontal currents. Such anomalous events in the inertial oscillations of the oceanic waters are probably typical of other steep shelves with dominant strong variable currents.

**SPELL OK**

## REFERENCES

1. V. G. Bondur, N. N. Filatov, and Yu. V. Grebenyuk, et al., *Oceanology* **47** (6) 769 (2007).
2. V. G. Bondur, Yu. V. Grebenyuk, and K. D. Sabinin, *Oceanology* **49** (3) 299 (2009).
3. V. Bondur, in *Proceedings of the 31st International Symposium on Remote Sensing of Environment, 2006* (ISRSE, St-Petersburg, 2006), p. 7.
4. V. Bondur, in *Waste Water—Evaluation and Management* (InTech, Croatia, 2011).
5. V. Bondur and M. Tsidilina, *Proceedings of the 31st International Symposium on Remote Sensing of Environment, 2006* (ISRSE, St-Petersburg, 2006), p. 192–195.
6. R. Keeler, V. Bondur, and C. Gibson, *Geophys. Res. Lett.* **32** L12610.
7. R. Keeler, V. Bondur, and D. Vithanage, *Sea Technol.* 53–58 (2004).
8. P. K. Kundu and R. E. Thompson, *J. Phys. Oceanogr.* **15** (8) (1985).
9. K. V. Konyaev and K. D. Sabinin, *Waves Inside the Ocean* (GIMIZ, St-Petersburg, 1992) [in Russian].
10. V. A. Rozhkov, *Methods of Probabilistic Analysis of Oceanological Processes* (Gidrometeoizdat, Leningrad, 1979) [in Russian].
11. S. Elipot, R. Lumpkin, and G. Prieto, *J. Geophys. Res.* **115** C09010 (2010).
12. P. Stoica and R. L. Moses, *Introduction to Spectral Analysis* (Prentice–Hall, Englewood Cliffs, NJ, 1997).